nature immunology

Protein kinase C-η controls CTLA-4–mediated regulatory T cell function

Kok-Fai Kong[1,9], Guo Fu[2,9], Yaoyang Zhang[3], Tadashi Yokosuka[4,5], Javier Casas[2], Ann J Canonigo-Balancio[1], Stephane Becart[1], Gisen Kim[6], John R Yates III[3], Mitchell Kronenberg[6], Takashi Saito[4], Nicholas R J Gascoigne[2,7,8,10] & Amnon Altman[1,10]

Regulatory T (T_{reg}) cells, which maintain immune homeostasis and self-tolerance, form an immunological synapse (IS) with antigen-presenting cells (APCs). However, signaling events at the T_{reg} cell IS remain unknown. Here we show that the kinase PKC-η associated with CTLA-4 and was recruited to the T_{reg} cell IS. PKC-η–deficient T_{reg} cells displayed defective suppressive activity, including suppression of tumor immunity but not of autoimmune colitis. Phosphoproteomic and biochemical analysis revealed an association between CTLA-4–PKC-η and the GIT2-αPIX-PAK complex, an IS-localized focal adhesion complex. Defective activation of this complex in PKC-η–deficient T_{reg} cells was associated with reduced depletion of CD86 from APCs by T_{reg} cells. These results reveal a CTLA-4–PKC-η signaling axis required for contact-dependent suppression and implicate this pathway as a potential cancer immunotherapy target.

The discovery and recognition of $CD4^+Foxp3^+$ T_{reg} cells as a distinct subset of T cells with immunoregulatory function is a major advance in our understanding of the immune system[1–3]. T_{reg} cells actively maintain immune homeostasis and self-tolerance, and one prominent T_{reg} cell–mediated suppressive mechanism is dependent on contact with APCs[4]. This physical contact promotes the formation of a specialized signaling platform, known as the IS, at the T_{reg} cell–APC interface.

CTLA-4 is a potent negative regulator of T cell–mediated immune responses through its actions in both T_{eff} and T_{reg} cells. CTLA-4 is highly expressed on T_{reg} cells[3], and this high expression, as well as the higher affinity of CTLA-4 for its CD80 (B7-1) and CD86 (B7-2) ligands in comparison with CD28 (ref. 5), is associated with predominant localization of CTLA-4 at the T_{reg} cell IS and, consequently, displacement of CD28 from the IS[6]. However, despite extensive studies of CTLA-4, little is known about the intracellular signaling pathways initiated upon CTLA-4 engagement by its ligands. The SHP-1, SHP-2 and PP2A phosphatases, which are binding partners of CTLA-4 (ref. 7), may account for the intrinsic inhibitory activity of CTLA-4 in T_{eff} cells, but a recent study had demonstrated that these phosphatases are not recruited to the T_{reg} cell IS together with CTLA-4 (ref. 6). Thus, how CTLA-4 exerts its signaling effects at the T_{reg} cell IS remains unknown.

The T_{reg} cell IS is distinguishable from the 'conventional' IS formed between naive or effector T (T_{eff}) cells and APCs in several respects. First, although the T cell antigen receptor (TCR) is present in the central supramolecular activation cluster in both types of IS, the costimulatory CD28 receptor is recruited to the T_{eff} cell IS, whereas CTLA-4 is present at the T_{reg} cell IS[6,8]. Second, PKC-θ is absent from the T_{reg} cell IS and, moreover, in contrast to the case in T_{eff} cells, it negatively regulates the function of T_{reg} cells[4]. Physical association of PKC-θ, mediated by its V3 domain, with the costimulatory CD28 receptor underlies its recruitment to the central supramolecular activation cluster and essential functions in driving the activation, proliferation and differentiation of T_{eff} cells[9]. Hence, the absence of PKC-θ in the T_{reg} cell IS suggests that TCR signaling events in these cells could differ considerably from those of T_{eff} cells. Nevertheless, proximal TCR signaling appears intact in T_{reg} cells, as indicated by the phosphorylation and activation of the TCR-stimulated signaling proteins TCR, Lck[10], PDK1 (ref. 11), LAT and PLC-γ1 (ref. 12), all of which have been implicated in the *in vitro* suppressive function of T_{reg} cells. Because of these findings and, in particular, the importance of the association between LAT and activated PLC-γ1 (ref. 12), which is required for the hydrolysis of phosphatidylinositol 4,5-bisphosphate ($PtdIns(4,5)P_2$) and generation of diacylglycerol (DAG), the PKC-activating second messenger, we hypothesized that DAG should be produced locally[13] upon formation of ISs in T_{reg} cells and, furthermore, that this would lead to recruitment of a PKC family member other than PKC-θ to the IS and to the activation of such a PKC species. This PKC may, in turn, positively regulate the function of T_{reg} cells.

[1]Division of Cell Biology, La Jolla Institute for Allergy and Immunology, La Jolla, California, USA. [2]Department of Immunology and Microbial Science, The Scripps Research Institute, La Jolla, California, USA. [3]Department of Chemical Physiology, The Scripps Research Institute, La Jolla, California, USA. [4]RIKEN Center for Integrative Medical Sciences, Yokohama, Japan. [5]PRESTO, Japan Science and Technology Agency, Saitama, Japan. [6]Division of Developmental Immunology, La Jolla Institute for Allergy and Immunology, La Jolla, California, USA. [7]Department of Microbiology, Yong Loo Lin School of Medicine, National University of Singapore, Singapore. [8]Present address: Yong Loo Lin School of Medicine, National University of Singapore, Singapore. [9]These authors contributed equally to this work. [10]These authors jointly directed this work. Correspondence should be addressed to A.A. (amnon@liai.org), N.R.J.G. (michead@nus.edu.sg) or K.-F.K. (kfkong@liai.org).

Received 18 December 2013; accepted 10 March 2014; published online 6 April 2014; corrected after print 2 May 2014; doi:10.1038/ni.2866

Here we show that, by analogy with the PKC-θ–CD28 interaction in T_{eff} cells, which promotes their activation and function[9], the CD28-related receptor CTLA-4, which is highly expressed on T_{reg} cells and is required for their suppressive function[14,15], physically recruits another member of the novel PKC (nPKC) subfamily, PKC-η, which localizes at the T_{reg} cell IS after stimulation. This association required phosphorylated serine residues in PKC-η and a conserved, membrane-proximal motif in the cytoplasmic tail of CTLA-4, respectively. Although development of T_{reg} cells and expression of typical T_{reg} cell markers were normal in PKC-η–deficient (*Prkch*$^{-/-}$) T_{reg} cells, these cells displayed a grossly impaired contact-dependent suppressive activity *in vitro* and *in vivo*, which was associated with a grossly defective activation of the transcription factors NFAT and NF-κB. Lastly, we show that defective activation of a focal adhesion complex consisting of the kinase PAK and two additional proteins, PAK-interacting exchange factor (PIX) and G protein–coupled receptor kinase-interacting protein 2 (GIT2), which was physically associated with CTLA-4 and PKC-η, was associated with reduced ability of *Prkch*$^{-/-}$ T_{reg} cells to serially engage APCs; this provides a potential mechanistic basis for the impaired suppressive activity of these cells. Therefore, strategies that interfere with this signaling pathway may be beneficial for inhibiting T_{reg} cell function in cancer and, hence, boosting the immune response against tumors.

RESULTS

Phospho-PKC-η interacts with CTLA-4 in the T_{reg} cell IS

By analogy to the interaction of PKC-θ with the CTLA-4–related costimulatory receptor CD28, which is critical for the activation of T_{eff} cells[9], we first tested whether any PKC isoform could physically interact with CTLA-4. Using T hybridoma cells, we found that CTLA-4 coimmunoprecipitated with a higher than normal molecular weight species of PKC-η (**Fig. 1a**), but not with any other T cell–expressed PKC isoforms (**Supplementary Fig. 1a**). We reasoned that the shift in molecular weight of PKC-η might be due to phosphorylation. Indeed, treatment with alkaline phosphatase partially reversed the shift of the higher-molecular-weight species of PKC-η and resulted in the appearance of a lower-molecular-weight species (**Fig. 1b**), which indicated that CTLA-4 interacts predominantly with phosphorylated PKC-η. We found phosphorylated PKC-η in unstimulated Foxp3$^+$ T_{reg} cells but not in naive T cells (**Fig. 1c**), despite the fact that expression of mRNA encoding PKC-η and PKC-η protein was not substantially different between T_{eff} cells and T_{reg} cells (**Supplementary Fig. 1b**). Using a T_{reg} cell–APC conjugation system and confocal microscopy, we observed that, relative to PKC-θ, PKC-η preferentially localized in the T_{reg} cell IS, where it partially colocalized with the TCR (**Fig. 1d**). We analyzed the relative intensity of the fluorescence signals of enhanced green fluorescent protein (eGFP)-tagged PKC-η or PKC-θ fusion proteins in the T_{reg} cell IS by calculating the intensity ratio in the IS versus the opposite T cell pole. About 15% (3/20) of imaged cells displayed preferential localization of PKC-θ in the IS (ratio ≥ 5), consistent with the observation that a similar percentage of cells in this population were FoxP3$^-$ (by intracellular staining), representing contaminating activated T_{eff} cells in the induced (i)T_{reg} cell culture. Among the remaining cells, the intensity ratios for PKC-η and PKC-θ were 2.84 ± 0.22 and 1.51 ± 0.18 (average ± s.e.m.; $P < 0.0001$, two-sided Student's *t*-test), respectively (data not shown). Taken together, these results indicate that phosphorylated PKC-η associates with CTLA-4 in T_{reg} cells and, furthermore, that PKC-η preferentially colocalizes with CTLA-4 in the IS.

Development of Foxp3$^+$ T_{reg} cells is independent of PKC-η

Given the critical role of CTLA-4 in contact-dependent T_{reg} cell suppressive function, which involves depletion of CD80 and CD86 from APCs[14,15], we next examined the CD4$^+$Foxp3$^+$ T_{reg} cell population in the lymphoid organs of *Prkch*$^{-/-}$ mice by intracellular Foxp3 staining. The number and frequency of CD4$^+$Foxp3$^+$ cells was not significantly altered in the thymi and spleens of *Prkch*$^{-/-}$ mice compared to *Prkch*$^{+/+}$ mice (**Fig. 2a**,**b** and **Supplementary Fig. 2a**). However, there was a consistent increase in the numbers of CD4$^+$Foxp3$^+$ T_{reg} cells in peripheral and mesenteric lymph nodes of these mice (**Fig. 2c**,**d**), which suggested that PKC-η is dispensable for *in vivo* development of CD4$^+$Foxp3$^+$ T cells. Cells that have been 'licensed' to become Foxp3$^+$ expressed similar levels of typical T_{reg} cell markers, including Foxp3, TCRβ, CTLA-4, CD25, immunomodulatory receptor GITR and CD44 (**Fig. 2e**–**j**). Thus, PKC-η is dispensable for natural (n)T_{reg} cell development *in vivo*, and for iT_{reg} cell differentiation *in vitro* as assessed by expression of typical T_{reg} cell markers (data not shown).

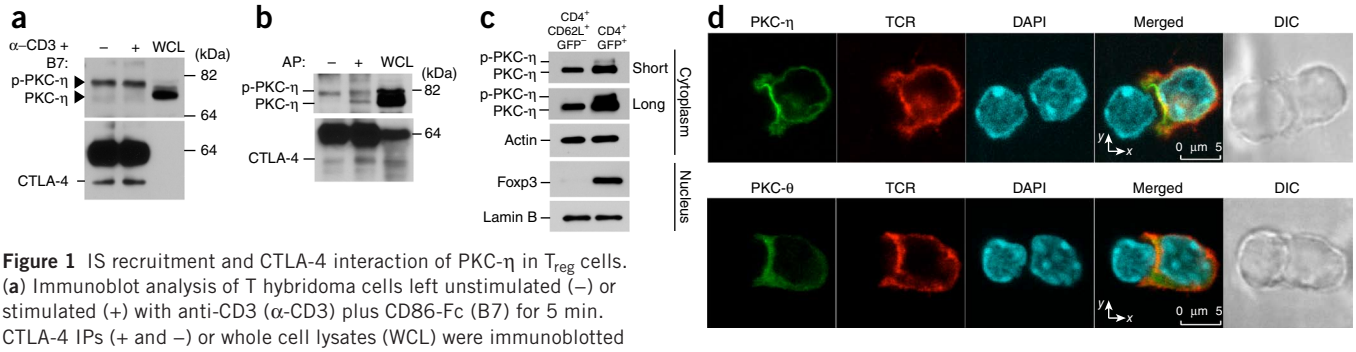

Figure 1 IS recruitment and CTLA-4 interaction of PKC-η in T_{reg} cells. (**a**) Immunoblot analysis of T hybridoma cells left unstimulated (–) or stimulated (+) with anti-CD3 (α-CD3) plus CD86-Fc (B7) for 5 min. CTLA-4 IPs (+ and –) or whole cell lysates (WCL) were immunoblotted with Abs to detect the indicated proteins. Arrowheads mark the two PKC-η species. p-PKC-η indicated phosphorylated PKC-η. (**b**) Immunoblot analysis of immunoprecipitates (IPs) or WCL from T hybridoma cells stimulated with anti-CD3 plus CD86-Fc for 5 min. CTLA-4 IPs were left untreated or treated with alkaline phosphatase (AP) before immunoblotting. (**c**) Immunoblot analysis of cytosol or nuclear fractions from sorted CD4$^+$CD62L$^+$GFP$^-$ (naive) and CD4$^+$GFP$^+$ (T_{reg}) cells (2 × 10^6 each) from *Prkch*$^{+/+}$ FIG mice. Long and short refer to long (10 min) or short (1 min) exposure times. (**d**) Confocal imaging of PKC-η (top) or PKC-θ (bottom) and TCRβ (TCR) localization in *in vitro* differentiated iT_{reg} cells from AND TCR-Tg *Rag2*$^{-/-}$ mice, which were retrovirally transduced with eGFP-tagged mouse PKC-θ or PKC-η 1 d after anti-CD3 and anti-CD28 stimulation. Sorted GFP$^+$ T cells (~90% FoxP3$^+$ by intracellular staining; data not shown) obtained on day 4 and stimulated for 5–10 min by conjugation with mouse cytochrome C–pulsed lipopolysaccharide-stimulated B cells were fixed and analyzed. eGFP-tagged PKC, TCR and nuclear DAPI staining are shown in green, red and blue, respectively. DIC, differential interference contrast. Data are representative of at least four experiments (**a**–**c**) and at least 100 cells collected from three independent experiments (**d**).

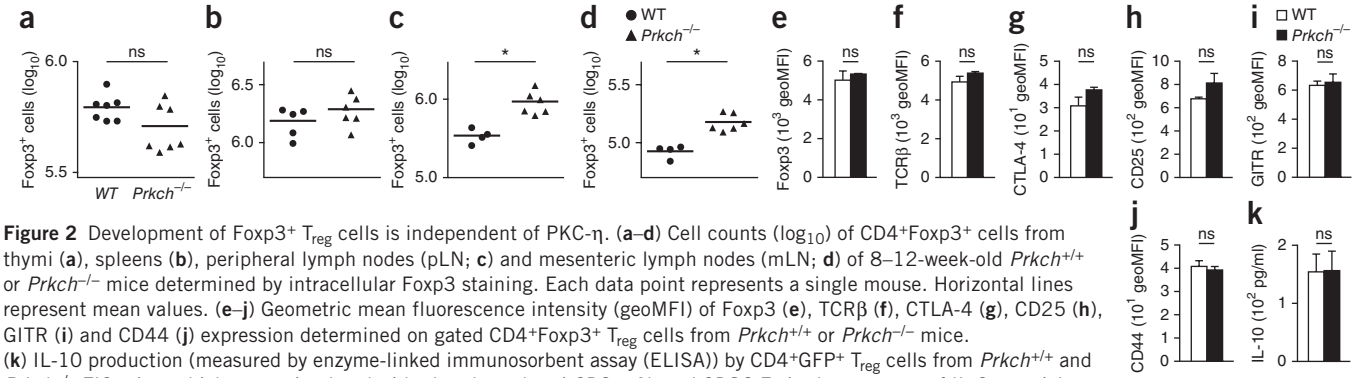

Figure 2 Development of Foxp3$^+$ T_{reg} cells is independent of PKC-η. (**a**–**d**) Cell counts (log_{10}) of CD4$^+$Foxp3$^+$ cells from thymi (**a**), spleens (**b**), peripheral lymph nodes (pLN; **c**) and mesenteric lymph nodes (mLN; **d**) of 8–12-week-old *Prkch*$^{+/+}$ or *Prkch*$^{-/-}$ mice determined by intracellular Foxp3 staining. Each data point represents a single mouse. Horizontal lines represent mean values. (**e**–**j**) Geometric mean fluorescence intensity (geoMFI) of Foxp3 (**e**), TCRβ (**f**), CTLA-4 (**g**), CD25 (**h**), GITR (**i**) and CD44 (**j**) expression determined on gated CD4$^+$Foxp3$^+$ T_{reg} cells from *Prkch*$^{+/+}$ or *Prkch*$^{-/-}$ mice. (**k**) IL-10 production (measured by enzyme-linked immunosorbent assay (ELISA)) by CD4$^+$GFP$^+$ T_{reg} cells from *Prkch*$^{+/+}$ and *Prkch*$^{-/-}$ FIG mice, which were stimulated with plate-bound anti-CD3 mAb and CD86-Fc in the presence of IL-2 overnight. Shown are mean ± s.e.m. ($n = 3$). ns, not significant; $^*P < 0.05$ (two-sided Student's *t*-test). Data are representative of three independent experiments.

PKC-η is required for Foxp3$^+$ T_{reg} cell suppressive function

We next explored the possibility that PKC-η might be required for the suppressive function of Foxp3$^+$ T_{reg} cells. To enable definitive identification of T_{reg} cells, we crossed *Prkch*$^{-/-}$ mice with mice coexpressing Foxp3 and enhanced GFP under the control of the endogenous *Foxp3* promoter (*Foxp3*-IRES-eGFP, where IRES is the internal ribosome entry site; hereafter called FIG)[16] to generate *Prkch*$^{-/-}$ FIG mice. We sorted CD4$^+$GFP$^+$ T_{reg} cells from *Prkch*$^{+/+}$ and *Prkch*$^{-/-}$ FIG mice, and found that, upon stimulation, they produced similar amount of interleukin 10 (IL-10; **Fig. 2k**), a cytokine that can mediate the suppressive activity of T_{reg} cells[17,18].

We next considered the possibility that, despite the presence of an apparently normal T_{reg} cell population in *Prkch*$^{-/-}$ mice, the suppressive activity of these cells may be defective. We first used a conventional *in vitro* T_{reg} cell suppression assay, which assessed the proliferation of naive T cells cocultured with T_{reg} cells and stimulated with anti-CD3 plus splenic dendritic cells (DCs) as an APC source. The percentage of dividing effector T (T_{eff}) cells was consistently greater in cultures with *Prkch*$^{-/-}$ T_{reg} cells compared to T_{eff} cells cocultured with *Prkch*$^{+/+}$ T_{reg} cells (**Fig. 3a**). The *Prkch*$^{-/-}$ T_{reg} cells were substantially impaired in their ability to suppress the proliferation of T_{eff} cells even at high T_{reg}/T_{eff} cell ratios, which indicated that PKC-η expression by T_{reg} cells is important for their function.

To determine the importance of PKC-η in T_{reg} cell function *in vivo*, we used two distinct experimental models, namely, homeostatic T cell population expansion and tumor growth. Transfer of naive CD4$^+$CD62L$^+$ T cells into immunodeficient mice leads to their massive proliferation, a process generally referred to as homeostatic expansion, although it is likely that some of this proliferation is antigen-driven[19]. T_{reg} cells control the population expansion of T_{eff} cells in a lymphopenic environment[20]. We adoptively transferred purified naive CD45.1$^+$CD4$^+$ T cells, either alone or in the presence of sorted *Prkch*$^{+/+}$ or *Prkch*$^{-/-}$ CD45.2$^+$CD4$^+$GFP$^+$ T_{reg} cells, into *Rag1*$^{-/-}$ mice, and determined T cell numbers 1 week after transfer. In the presence of *Prkch*$^{+/+}$ T_{reg} cells, CD45.1$^+$ T_{eff} cell numbers were significantly reduced in all secondary lymphoid organs we examined; in contrast, we observed minimal or no reduction in T_{eff} cell population expansion in the presence of *Prkch*$^{-/-}$ T_{reg} cells (**Fig. 3b**–**d**). Similar numbers of *Prkch*$^{+/+}$ and *Prkch*$^{-/-}$ T_{reg} cells were present in these tissues (**Supplementary Fig. 2b**).

We next investigated the ability of *Prkch*$^{-/-}$ T_{reg} cells to inhibit the immune response against a growing tumor. We adoptively transferred splenocytes, depleted of CD25$^+$ T cells, into *Rag1*$^{-/-}$ mice as a source of T_{eff} cells in the absence or presence of T_{reg} cells 1 d before inoculation of B16-F10 melanoma cells[14,21]. Transfer of CD25$^+$ T cell–depleted splenocytes alone resulted in relatively small skin tumors, whereas mice receiving T_{eff} cells together with *Prkch*$^{+/+}$ T_{reg} cells developed

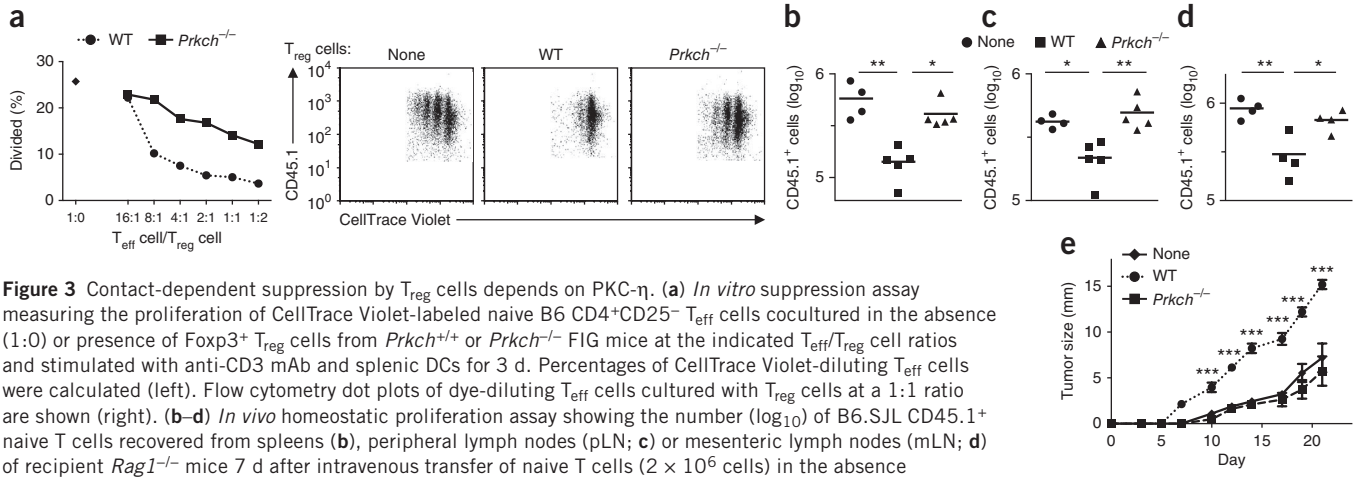

Figure 3 Contact-dependent suppression by T_{reg} cells depends on PKC-η. (**a**) *In vitro* suppression assay measuring the proliferation of CellTrace Violet-labeled naive B6 CD4$^+$CD25$^-$ T_{eff} cells cocultured in the absence (1:0) or presence of Foxp3$^+$ T_{reg} cells from *Prkch*$^{+/+}$ or *Prkch*$^{-/-}$ FIG mice at the indicated T_{eff}/T_{reg} cell ratios and stimulated with anti-CD3 mAb and splenic DCs for 3 d. Percentages of CellTrace Violet-diluting T_{eff} cells were calculated (left). Flow cytometry dot plots of dye-diluting T_{eff} cells cultured with T_{reg} cells at a 1:1 ratio are shown (right). (**b**–**d**) *In vivo* homeostatic proliferation assay showing the number (log_{10}) of B6.SJL CD45.1$^+$ naive T cells recovered from spleens (**b**), peripheral lymph nodes (pLN; **c**) or mesenteric lymph nodes (mLN; **d**) of recipient *Rag1*$^{-/-}$ mice 7 d after intravenous transfer of naive T cells (2×10^6 cells) in the absence (none) or presence of CD4$^+$GFP$^+$ T_{reg} cells (0.5×10^6 cells) sorted by flow cytometry from *Prkch*$^{+/+}$ or *Prkch*$^{-/-}$ FIG mice. Each data point represents a single mouse. Horizontal lines represent mean values. (**e**) Sequential measurements of B16-F10 melanoma growth in groups of *Rag1*$^{-/-}$ mice, which received CD25-depleted B6 splenic cells (1.5×10^7 cells; a source of T_{eff} cells) without ($n = 6$) or with 0.5×10^6 CD4$^+$GFP$^+$ T_{reg} cells from *Prkch*$^{+/+}$ ($n = 8$) or *Prkch*$^{-/-}$ ($n = 6$) FIG mice, and were inoculated 1 d later with tumor cells (2×10^5 cells). Tumor diameters along two perpendicular axes were measured 2–3 times per week. Shown are mean ± s.e.m. analyzed by analysis of variance (ANOVA) with post hoc Bonferroni's corrections. $^*P < 0.05$; $^{**}P < 0.01$; $^{***}P < 0.001$. Data are representative of at least five (**a**) and at least three (**b**–**e**) independent experiments.

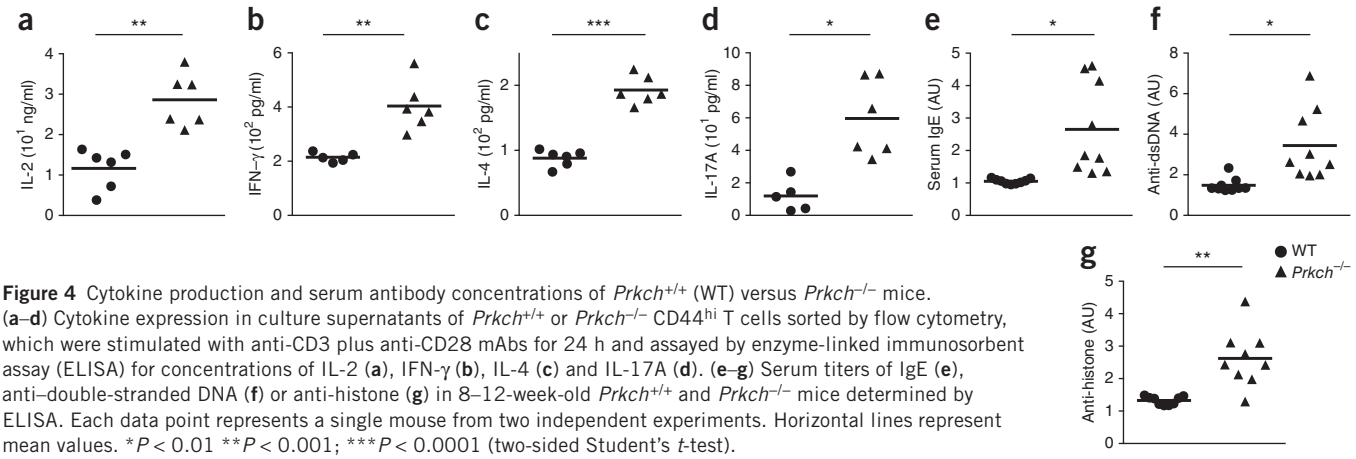

Figure 4 Cytokine production and serum antibody concentrations of *Prkch*$^{+/+}$ (WT) versus *Prkch*$^{-/-}$ mice. (**a**–**d**) Cytokine expression in culture supernatants of *Prkch*$^{+/+}$ or *Prkch*$^{-/-}$ CD44^{hi} T cells sorted by flow cytometry, which were stimulated with anti-CD3 plus anti-CD28 mAbs for 24 h and assayed by enzyme-linked immunosorbent assay (ELISA) for concentrations of IL-2 (**a**), IFN-γ (**b**), IL-4 (**c**) and IL-17A (**d**). (**e**–**g**) Serum titers of IgE (**e**), anti–double-stranded DNA (**f**) or anti-histone (**g**) in 8–12-week-old *Prkch*$^{+/+}$ and *Prkch*$^{-/-}$ mice determined by ELISA. Each data point represents a single mouse from two independent experiments. Horizontal lines represent mean values. $*P < 0.01$ $**P < 0.001$; $***P < 0.0001$ (two-sided Student's *t*-test).

massive B16 tumors, which reflected inhibition of the T_{eff} cell antitumor response by the cotransferred T_{reg} cells (**Fig. 3e**). Cotransfer of *Prkch*$^{-/-}$ T_{reg} cells resulted in substantially reduced tumor growth, similar to that seen in mice receiving only T_{eff} cells (**Fig. 3e**). Taken together, these results indicate that in the absence of PKC-η, the *in vivo* suppressive function of T_{reg} cells is attenuated, which leads to enhanced homeostatic proliferation and antitumor immunity.

Consistent with the importance of PKC-η in T_{reg} cell suppressive functions, *Prkch*$^{-/-}$ mice exhibit lymphadenopathy, reflected by increased numbers of T cells and B cells, as well as a higher proportion of CD44^{hi} T cells, characteristic of an activated phenotype[22]. Indeed, *Prkch*$^{-/-}$ CD44^{hi} T cells secreted significantly elevated amounts of effector cytokines, including IL-2, IFN-γ, IL-4 and IL-17A (**Fig. 4a**–**d**), upon *in vitro* stimulation with anti-CD3 plus anti-CD28 monoclonal antibodies (mAbs). Consistent with this hyperactive phenotype, *Prkch*$^{-/-}$ mice displayed elevated serum titers of IgE (**Fig. 4e**) and autoantibodies against double-stranded DNA and histone (**Fig. 4f**,**g**) at 8–12 weeks of age, which implies that the immune system is deregulated and hyperactive in the absence of PKC-η.

We also assessed the ability of *Prkch*$^{+/+}$ and *Prkch*$^{-/-}$ T_{reg} cells to inhibit the development of autoimmune colitis in an established T cell transfer model. Although transfer of naive T cells alone into *Rag1*$^{-/-}$ recipient mice induced weight loss, indicative of the development of chronic inflammatory bowel disease, cotransfer of either *Prkch*$^{+/+}$ or *Prkch*$^{-/-}$ GFP$^+$ T_{reg} cells protected the recipients against weight loss (**Supplementary Fig. 3a**) and inhibited the population expansion of T_{eff} (CD45.1$^+$) cells (**Supplementary Fig. 3b**). Thus, despite the *in vitro* (**Fig. 3a**) and *in vivo* (**Fig. 3b**–**e**) severe defects in their suppressive function, *Prkch*$^{-/-}$ T_{reg} cells were still able to protect, albeit perhaps incompletely, recipient mice against the development of colitis. This finding suggests that in this particular disease model, *Prkch*$^{-/-}$ T_{reg} cells use an alternative, PKCη-independent suppressive mechanism(s), e.g., IL-10–mediated suppression (**Fig. 2k**). Furthermore, increased proliferation (or localization) of *Prkch*$^{-/-}$ T_{reg} cells in the inflammatory bowel environment may compensate for their defective intrinsic suppressive function. Indeed, we found greater numbers of cotransferred *Prkch*$^{-/-}$ T_{reg} cells relative to *Prkch*$^{+/+}$ T_{reg} cells in the secondary lymphoid organs of the recipient mice, and this effect tended to be more pronounced in mesenteric lymph nodes, which drain the site of inflammation (**Supplementary Fig. 3c**). Together, these findings suggest that PKC-η is not globally required for all forms of T_{reg} cell–induced suppression, and that it is dispensable for T_{reg} cell–mediated inhibition of colitis.

Mapping and importance of CTLA-4–PKC-η interaction

The predominant association of phosphorylated PKC-η with CTLA-4 in T_{reg} cells suggested that phosphorylated residues mediate this interaction. To pinpoint potential phosphorylation site(s) in PKC-η required for its interaction with CTLA-4, we created mutant vectors encoding PKC-η with substitutions in six predicted phosphorylation sites, transfected these mutant vectors into JTAg cells, a Jurkat cell derivative that does not express CD28, along with a vector encoding full-length CTLA-4, and immunoprecipitated the transfected CTLA-4 proteins. Upon costimulation with anti-CD3 mAb and CD86-Fc recombinant protein, we found that mutations of amino acids Ser28 and Ser32 in the C2 domain, or Ser317 in the V3 domain of PKC-η abolished the interaction with CTLA-4; as a control, substitution of three other phosphorylation sites (Ser327, Thr656 or Ser675) did not affect this interaction (**Fig. 5a**). Thus, phosphorylation of Ser28 and Ser32 or Ser317 in PKC-η is critical for the interaction with CTLA-4.

To determine whether the association between PKC-η and CTLA-4 is required for the suppressive function of T_{reg} cells, we generated bone marrow (BM) chimeric mice by retrovirally reconstituting *Prkch*$^{-/-}$ FIG BM cells with wild-type PKC-η or a mutant that does not interact with CTLA-4, PKC-η(S28A,S32A). The retroviral vector used coexpressed a nonsignaling rat CD2 (rCD2) to allow isolation of transduced T cells. We sorted transduced T_{reg} cells (rCD2$^+$GFP$^+$CD45.2$^+$) from chimeric mice and assayed them for their ability to suppress the *in vivo* homeostatic proliferation of cotransferred naive CD45.1$^+$ T cells. Unlike T_{reg} cells expressing wild-type PKC-η, T_{reg} cells reconstituted with PKC-η(S28A,S32A) were incapable of suppressing naive T cell proliferation in the spleens and lymph nodes of adoptively transferred recipients (**Fig. 5b**–**d**).

To map the critical motif in the cytoplasmic tail of CTLA-4 that is required for the interaction with PKC-η, we substituted four conserved tail residues, i.e., a membrane-proximal positively charged motif (K^{188}XXKKR^{193}, where X is any amino acid other than K or R), a proline-rich motif (Pro205,Pro206,Pro209) and two tyrosine residues (Tyr201 or Tyr218). We found that mutation of the positively charged K^{188}XXKKR^{193} motif as well as complete deletion of the CTLA-4 cytoplasmic tail (deletion of amino acids 183–223; Δ183–223) greatly reduced the association with PKC-η; in contrast, substitution of the conserved tyrosine residues or the proline-rich motif did not affect the interaction (**Fig. 5e**). This membrane-proximal motif is highly conserved throughout evolution from fish to primates (**Supplementary Fig. 4a**). Partial truncation of the cytoplasmic tail of CTLA-4 (Δ192–223), which

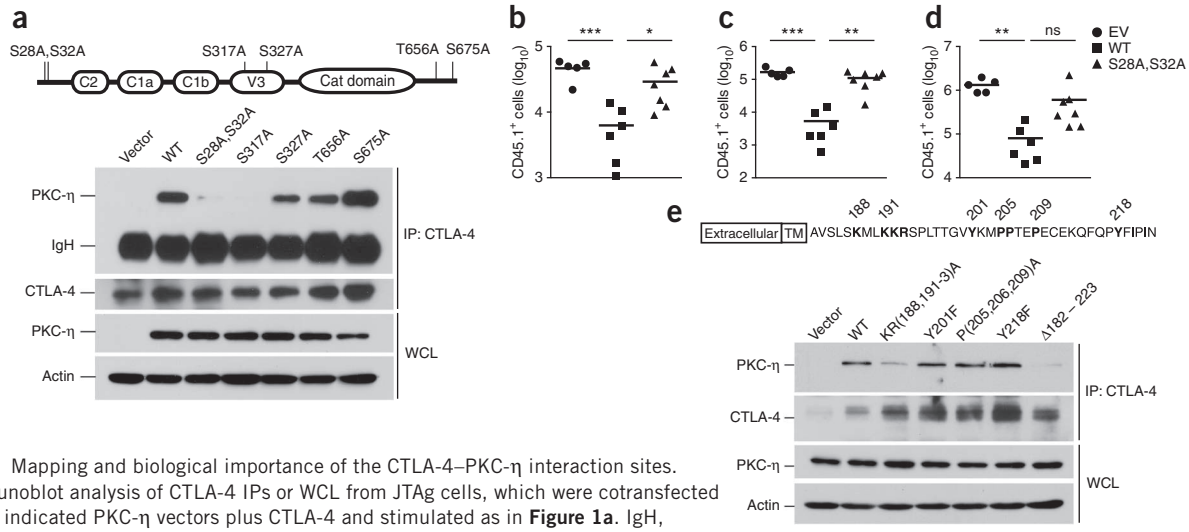

Figure 5 Mapping and biological importance of the CTLA-4–PKC-η interaction sites. (**a**) Immunoblot analysis of CTLA-4 IPs or WCL from JTAg cells, which were cotransfected with the indicated PKC-η vectors plus CTLA-4 and stimulated as in **Figure 1a**. IgH, heavy chain of the precipitating antibody. Schematic at the top shows human PKC-η and its phosphorylation sites that were substituted in this work. (**b**–**d**) *In vivo* homeostatic proliferation assay performed as described in **Figure 3b–d** showing the number (log_{10}) of B6.SJL CD45.1$^+$ naive T cells, which were recovered from spleens (**b**), peripheral lymph nodes (pLN; **c**) or mesenteric lymph nodes (mLN; **d**) of recipient *Rag1*$^{-/-}$ mice 10 d after intravenous transfer of naive cells (2×10^6 cells) in the absence (vector) or presence of rCD2$^+$CD4$^+$GFP$^+$ T_{reg} cells (0.5×10^6 cells) sorted by flow cytometry. T_{reg} cells were derived from *Prkch*$^{-/-}$ BM mouse chimeras reconstituted with wild-type PKC-η (WT) or a CTLA-4 noninteracting PKC-η(S28A,S32A) using retroviral pMIG-IRES-rCD2 vector. Each data point represents a single mouse, and the horizontal lines represent the mean values. EV, empty vector. Data were analyzed by ANOVA with post hoc Bonferroni's corrections. ns, not significant; $*P < 0.05$; $**P < 0.01$; $***P < 0.001$. (**e**) Immunoblot analysis of CTLA-4 IPs or WCL from JTAg cells cotransfected with the indicated CTLA-4 vectors plus wild-type PKC-η, and processed as in **a**. Schematic representation of mouse CTLA-4 is shown on top. Residues in bold were substituted in this work. Data are representative of at least five independent experiments (**a**,**e**) and two independent experiments (**b**–**d**).

left intact nine membrane-proximal residues, including Lys188 and Lys191, resulted in a residual association with PKC-η, which, however, was weaker than that displayed by full-length CTLA-4 (**Supplementary Fig. 4b**). T_{reg} cells expressing CTLA-4 with a similar incomplete truncation of the cytoplasmic tail have been reported to retain suppressive activity[23,24]. We also found that the interaction between CTLA-4 and PKC-η was not affected by PP2, an inhibitor of Src-family kinases (data not shown), consistent with the lack of effect of Tyr201 or Tyr218 substitutions in CTLA-4 tail on this interaction. Taken together, these results reveal that the CTLA-4–PKC-η interaction is necessary for the suppressive function of T_{reg} cells, thereby implicating PKC-η in a signaling axis linking CTLA-4 to T_{reg} cell–mediated suppression.

Impaired CD86 depletion by *Prkch*$^{-/-}$ T_{reg} cells

In comparison to T_{eff} cells, T_{reg} cells preferentially form aggregates with APCs[4,25], and this is due in part to the higher expression of adhesion molecules such as LFA-1 (ref. 26) and neuropilin-1 (ref. 27) on T_{reg} cells. Such T_{reg} cell–APC engagement has been implicated as a potential suppression mechanism, as it allows T_{reg} cells to effectively compete with T_{eff} cells in engaging APCs and, thus, inhibit T_{eff} cell activation[25]. However, activation of LFA-1 and its conversion to a high-affinity state, as measured by adhesion to its ligand, ICAM-1, was intact in *Prkch*$^{-/-}$ T_{reg} cells (**Supplementary Fig. 5**). *Prkch*$^{+/+}$ and *Prkch*$^{-/-}$ T_{reg} cells expressed similar amounts of neuropilin-1, CD39 and CD73 (data not shown); the latter two are cell-surface molecules that have been implicated in T_{reg} cell–mediated suppression through an adenosine-dependent action[28].

To elucidate the signaling mechanism potentially responsible for the PKC-η–mediated suppression, we performed a phosphoproteomic analysis of *Prkch*$^{+/+}$ versus *Prkch*$^{-/-}$ T_{reg} cells and found that PAK2 and GIT2, two components of a focal adhesion complex that promotes focal adhesion disassembly and, hence, cellular motility[29,30], were substantially hypophosphorylated in *Prkch*$^{-/-}$ T_{reg} cells (**Supplementary Fig. 6a**). A complex of these two proteins together with the guanine nucleotide exchange factors αPIX or βPIX has been found to translocate to the T cell IS and to be required for optimal T_{eff} cell activation[31]. Moreover, CTLA-4 immunoprecipitates from anti-CD3– plus anti–CTLA-4–costimulated *Prkch*$^{+/+}$ T_{reg} cells contained not only PKC-η but also GIT2, αPIX and PAK (**Fig. 6a**). These proteins were also present in PKC-η immunoprecipitates (data not shown). Of note, recruitment of this complex was unique to CTLA-4 costimulation, because the association of the GIT2-αPIX-PAK complex with CTLA-4 was barely above background level when the cells were costimulated with anti-CD3 plus anti-CD28 mAbs (**Supplementary Fig. 6b**). Thus, this particular signaling event is not shared between CTLA-4 and CD28. Furthermore, the activating phosphorylation of PAK kinases was severely reduced in *Prkch*$^{-/-}$ T_{reg} cells (**Fig. 6b**), which indicated impaired activation of this complex.

Given the impaired activation of PAK, and because PAK was found to be required for TCR-induced transcriptional activation of NFAT and the CD28 response element (which includes an NF-κB binding site) in Jurkat T cells[31,32], we also examined whether *Prkch*$^{-/-}$ T_{reg} cells display impaired activation of these transcription factors after costimulation with anti-CD3ε plus anti–CTLA-4 mAbs. In these conditions, we observed a severe defect in NFATc1 and NF-κB activation in the *Prkch*$^{-/-}$$T_{reg}$ cells (**Fig. 6c**).

Because the GIT-PIX-PAK complex promotes cellular motility through focal adhesion disassembly[29,30], we investigated whether the defective activation of the GIT2-αPIX-PAK complex in *Prkch*$^{-/-}$ T_{reg} cells might result in a more stable conjugation of *Prkch*$^{-/-}$ T_{reg} cells with APCs. We noticed that the efficiency of conjugation between *Prkch*$^{-/-}$ T_{reg} cells and APCs was significantly higher by comparison to APC conjugates of *Prkch*$^{+/+}$ T_{reg} cells (**Fig. 6d**), suggesting that in *Prkch*$^{-/-}$

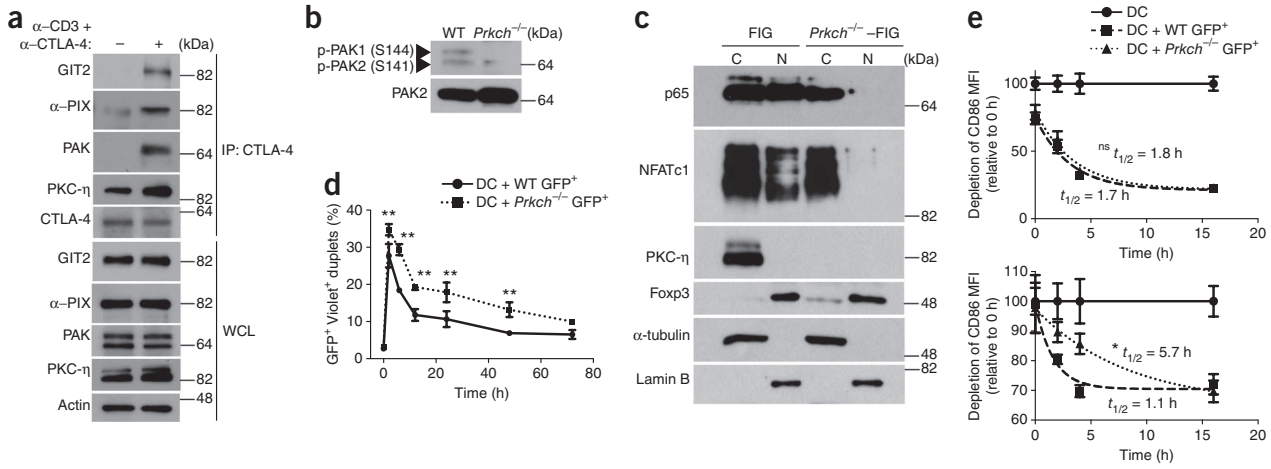

Figure 6 CTLA-4–PKC-η recruits GIT2-αPIX-PAK complex and modulates T_{reg} cell–APC interaction. (**a**) Immunoblot analysis of CTLA-4 IPs or WCL from flow cytometry–sorted *Prkch*$^{+/+}$ FIG CD4$^+$GFP$^+$ T_{reg} cells, which were left unstimulated (–) or stimulated (+) with anti-CD3ε plus anti–CTLA-4 mAbs for 5 min. (**b**) Expression of phospho-PAK1, phospho-PAK2 and total PAK2 in lysates of CD4$^+$GFP$^+$ T_{reg} cells from *Prkch*$^{+/+}$ or *Prkch*$^{-/-}$ FIG mice determined by immunoblotting with antibodies to indicated proteins. (**c**) Immunoblot analysis of cytosolic (C) and nuclear (N) fractions from cell lysates of flow cytometry–sorted GFP$^+$ T_{reg} cells derived from *Prkch*$^{+/+}$ (FIG) or *Prkch*$^{-/-}$ FIG mice, which were stimulated with anti-CD3 plus anti–CTLA-4 antibodies for 5 min. (**d**) Conjugation assay measuring formation of cell doublets between flow cytometry–sorted CD4$^+$GFP$^+$ *Prkch*$^{+/+}$ or *Prkch*$^{-/-}$ FIG T_{reg} and CellTrace Violet–labeled splenic DCs at different times during a 3 d coculture period in the presence of anti-CD3 mAb and IL-2. Percentages of GFP$^+$ and Violet$^+$ double-positive doublets are shown. Shown are mean ± s.e.m.; analyzed with two-sided Student's *t*-test. $*P < 0.05$; $**P < 0.001$. (**e**) CD86 depletion from APCs cocultured in the absence (DC) or presence of flow cytometry–sorted CD4$^+$GFP$^+$ *Prkch*$^{+/+}$ (DC + WT GFP$^+$) or *Prkch*$^{-/-}$ (DC + *Prkch*$^{-/-}$ GFP$^+$) FIG T_{reg} cells. A first set of CD45.2$^+$ splenic DCs was cultured for 9 h in the presence of anti-CD3 mAb and IL-2 before the addition of a second set of CD45.1$^+$ splenic DCs. The geometric mean fluorescence intensity (MFI) of CD86 was determined on gated CD11c$^+$ Annexin V$^-$ CD45.2$^+$ (top) and CD11c$^+$ Annexin V$^-$ CD45.1$^+$ (bottom) cells, respectively. The $t_{1/2}$ values of CD86 decay curves were calculated using the GraphPad Prism program. Data are representative of three independent experiments. Shown are mean ± s.e.m.; analyzed with two-sided Student's *t*-test. ns, not significant; $*P < 0.05$.

T_{reg} cells impaired activation of the GIT2-αPIX-PAK complex leads to defective breaking of T_{reg} cell–APC contacts.

If *Prkch*$^{-/-}$$T_{reg}$ cells display impaired dissociation from engaged APCs because of defective activation of the GIT2-αPIX-PAK complex, this defect may be expected to translate into reduced ability of *Prkch*$^{-/-}$ T_{reg} cells to serially engage new APCs, which, in turn, could result in reduced suppressive activity. This prediction is based on findings that T_{reg} cells can capture CD80 and CD86 from APCs, a process that depletes the ligands required for CD28 costimulation of T_{eff} cells[15] and is thus a potential mechanism of contact-dependent T_{reg} cell–mediated suppression. To address this possibility, we tested the ability of *Prkch*$^{+/+}$ versus *Prkch*$^{-/-}$ T_{reg} cells to deplete CD86 from cocultured CD45.2$^+$CD11c$^+$ APCs as an indirect measure of APC engagement by the T_{reg} cells. *Prkch*$^{+/+}$ and *Prkch*$^{-/-}$ T_{reg} cells were equally capable of depleting CD86 from these APCs (**Fig. 6e**). However, upon subsequent addition of a second pool of APCs, distinguished from the first APC population by their CD45.1 expression, *Prkch*$^{-/-}$ T_{reg} cells had a significant delay in their ability to deplete CD86 from these newly introduced APCs, as indicated by the fact that it took them about fourfold longer (~16 h versus ~4 h) to execute the same level of CD86 depletion as that accomplished by *Prkch*$^{+/+}$ T_{reg} cells (**Fig. 6e**). This observation supports the notion that the relative inefficiency of *Prkch*$^{-/-}$ T_{reg} cells in serially engaging new APCs and, hence, in effectively depleting APC-expressed CD86, could account, at least in part, for their reduced suppressive activity. Our findings imply that a T_{reg} cell–intrinsic signaling mechanism dependent on CTLA-4–PKC-η is required in order to manifest the cell-extrinsic suppressive function of CTLA-4 toward T_{eff} cells.

DISCUSSION

We report an interaction of CTLA-4 with PKC-η and preferential IS localization of PKC-η in T_{reg} cells upon their activation. Moreover, PKC-η and its CTLA-4 association were required for the contact-dependent suppressive function of T_{reg} cells, albeit not for their development. Although *Prkch*$^{-/-}$ T_{reg} cells displayed defective suppressive activity in a conventional *in vitro* suppression assay, and in *in vivo* homeostatic proliferation and antitumor immunity models, they could still inhibit the development of autoimmune colitis. Our findings provide two potential explanations for these apparently discrepant observations. First, enhanced expansion of *Prkch*$^{-/-}$ T_{reg} cells in the inflammatory bowel environment, which was particularly noticeable in mesenteric lymph nodes of recipient mice, could compensate for the reduced intrinsic suppressive function of these cells. Second, T_{reg} cells use various mechanisms of suppression, and the relative importance of each mechanism depends on the environment and the context of the immune response. For example, similar to *Prkch*$^{-/-}$ T_{reg} cells, *Ctla4*$^{-/-}$ T_{reg} cells suppress the development of colitis through intact compensatory expression of IL-10 (ref. 33), and we found that *Prkch*$^{-/-}$ T_{reg} cells expressed normal amounts of IL-10. Thus, the CTLA-4–associated PKC-η–dependent suppressive pathway that we describe here may be less relevant in T_{reg} cell suppressive mechanisms that do not depend on T_{reg} cell–APC contact but, rather, on soluble mediators. If our observations of a dispensable role of PKC-η in T_{reg} cell protection against colitis can be extended to other autoimmune disease models, this would suggest that strategies that selectively inhibit PKC-η or its association with CTLA-4 may disable T_{reg} cells from inhibiting antitumor immunity without affecting the ability

of these T_{reg} cells to protect against autoimmune diseases, a notion with important potential translational implications.

The T_{reg} cell defect revealed by our study may explain the increased cytokine production and higher amounts of serum IgE and autoantibodies in *Prkch*$^{-/-}$ mice, although intrinsic hyperactivity of the T_{eff} cells in these mice could also contribute to this increase. Nevertheless, it is interesting to note that mice with a T_{reg} cell–specific deletion of *Ctla4* display similar increases in cytokine, IgE and autoantibody amounts[14], which reinforces the notion of a functionally relevant link between CTLA-4 and PKC-η at the level of T_{reg} cell–mediated suppression.

The recruitment of a GIT2-αPIX-PAK complex to CTLA-4 (and PKC-η) upon TCR plus CTLA-4 (but not CD28) costimulation of T_{reg} cells and its impaired activation in *Prkch*$^{-/-}$ T_{reg} cells suggest a potential mechanism underlying their impaired suppressive activity, based on previous findings that this macromolecular complex is required for the disassembly of focal adhesions in neurons and epithelial cells[29,30]. Given the reported localization of this complex to the T cell IS and its importance for activation of T cells[31], it is possible that the TCR-activated GIT2-αPIX-PAK complex destabilizes T cell–APC contacts, thereby promoting conversion of the mature, concentric IS into an unstable IS (i.e., kinapse), which is important for the motility of T cells and their ability to serially engage new APCs[34]. In the context of contact-dependent, T_{reg} cell–mediated suppression, increased stability of T_{reg} cell–APC conjugates and the concomitant reduction in their ability to serially engage new APCs would be translated to impaired overall suppressive activity. Consistent with this notion, we found that *Prkch*$^{-/-}$$T_{reg}$ cells form more efficient contacts with APCs in comparison with their *Prkch*$^{+/+}$ counterparts and, furthermore, these *Prkch*$^{-/-}$ T_{reg} cells displayed a reduced ability to deplete CD86 from a second set of added APCs, likely a reflection of impairment in their disengagement from the first set of APCs. When considered at the population level and the relatively long time during which T_{reg} cells have the opportunity to engage APCs, this effect could translate into an overall reduction in depletion of CD86 and, consequently, reduced suppression of T_{reg} cells. Hence, our findings identify a T_{reg} cell–intrinsic signaling mechanism consisting of a CTLA-4–bound PKC-η–GIT2-αPIX-PAK complex, which has a role in promoting the cell-extrinsic suppressive function of T_{reg} cell–expressed CTLA-4 on T_{eff} cells.

The biology of CTLA-4 is complex and its mechanisms of action in T cells are still incompletely understood. This complexity reflects, to a large extent, the fact that CTLA-4 is expressed both in T_{eff} cells where it functions in a cell-autonomous manner in *cis* to inhibit their activation, and in T_{reg} cells where it operates in a cell-nonautonomous manner in *trans* to dampen responses of T_{eff} cells[17,18,35]. Earlier studies did not distinguish between these functions, but with the conditional deletion of *Ctla4* in T_{reg} cells only, it became evident that expression of CTLA-4 by T_{reg} cells is in most (but not all) cases important for their suppressive function through depletion of CD80 and CD86 from APCs[14,15,36].

Ctla4$^{-/-}$ mice display fatal lymphoproliferative disorder characterized by the systemic infiltration of pathogenic self-reactive T cells[37,38]. Although *Prkch*$^{-/-}$ mice displayed moderate lymphadenopathy, increase in memory-activated T cells and cytokine expression, and elevated IgE and autoantibodies at a relatively young age, they lived into adulthood (~1 year) with no gross signs of pathology (data not shown). Several functional disparities could account for these different phenotypes. First, CTLA-4 inhibits thymocyte negative selection[39], and, as a result, *Ctla4*$^{-/-}$ mice harbor autoreactive T cells that cause tissue damage[40]. However, thymic selection is largely intact in the absence of PKC-η[22], which suggests that the lack of overt autoreactivity and lymphoproliferation in *Prkch*$^{-/-}$ mice might limit the self-destructive nature of the hyperactive *Prkch*$^{-/-}$ T_{eff} cells. Second, the inhibitory effect of CTLA-4 is mediated by a combination of non–mutually exclusive mechanisms consisting of T_{reg} cell–intrinsic as well as T_{eff} cell–intrinsic mechanisms, and both mechanisms can cooperate to dampen T_{eff} cell responses. Third, our findings strongly suggest that the intrinsic ability *Prkch*$^{-/-}$ T_{reg} cells to deplete CD86 from APCs by transendocytosis (which depends on the CTLA-4 extracellular domain) is intact, and that only the newly described signaling function of CTLA-4, i.e., the dissociation of T_{reg} cells from APCs mediated by the PKC-η–GIT2-αPIX-PAK complex (which depends on the CTLA-4 cytoplasmic domain) is impaired. In contrast, T_{reg} cells from germ-line *Ctla4*$^{-/-}$ mice or *Foxp3*-Cre conditional *Ctla4*$^{-/-}$ mice lack both of these CTLA-4 functions.

Our findings of altered APC engagement and presumed reduced motility of *Prkch*$^{-/-}$ T_{reg} cells may be related to the reported ability of CTLA-4 to reverse the TCR stop signal and promote the motility of T_{eff} cells, possibly via LFA-1 activation[41,42]. In contrast, T_{reg} cells have been found to be resistant to the CTLA-4–induced reversal of the TCR stop signal, which results in longer contact times with APCs[43], a scenario that would lead to lower overall T_{reg} cell motility and less frequent serial encounters with new APCs. However, we did not observe a defect in LFA-1 expression or activation in *Prkch*$^{-/-}$ T_{reg} cells; furthermore, although LFA-1 promotes the formation of a stable IS, our findings point to a defect at a later stage, i.e., disassembly of the IS in the *Prkch*$^{-/-}$ T_{reg} cells.

Clinical use of anti–CTLA-4 heralded a new era of cancer immunotherapy by targeting immunosuppression[44]. In many tumor tissues, infiltrating T_{reg} cells restrict the function of T_{eff} cells and, therefore, inhibiting critical T_{reg} cell signaling molecules that are important for their function could lead to enhanced antitumor responses[45]. Here we showed that phosphorylated PKC-η is recruited to the T_{reg} cell IS and is associated with the cytoplasmic tail of CTLA-4, and demonstrated the critical importance of this association for the contact-dependent suppressive activity of T_{reg} cells. Hence, the CTLA-4–PKC-η axis could represent a key therapeutic target for T_{reg} cell–dependent suppression in controlling cancer.

METHODS

Methods and any associated references are available in the online version of the paper.

Note: Any Supplementary Information and Source Data files are available in the online version of the paper.

ACKNOWLEDGMENTS

We acknowledge H. Cheroutre and Y.-C. Liu for helpful discussions, the excellent services provided by members of the Flow Cytometry Core Unit at the La Jolla Institute for Allergy and Immunology, as well as the Animal Husbandry Units at LIAI and the Scripps Research Institute. This is publication number 1552 from the La Jolla Institute for Allergy and Immunology and 21923 from The Scripps Research Institute. This work was supported by US National Institutes of Health grants CA35299 (A.A.), GM065230 (N.R.J.G.) and P01AI089624 (M.K.). K.-F.K. was supported by LIAI-T1D-CRF 2012 Fellowship and Young Investigator Award #270056 from the Melanoma Research Alliance.

AUTHOR CONTRIBUTIONS

K.-F.K. and G.F. designed experiments, collected data, performed analyses and wrote the paper; J.C., T.Y. and T.S. performed microscopy experiment; A.J.C.-B. was involved in experiments and data collection; S.B. performed and assisted in melanoma studies; Y.Z. and J.R.Y. did the phosphoproteomic experiments and analyses; G.K. and M.K. provided critical reagents and were involved in study design; N.R.J.G. and A.A. designed the study, analyzed data and wrote the paper.

COMPETING FINANCIAL INTERESTS
The authors declare no competing financial interests.

Reprints and permissions information is available online at http://www.nature.com/reprints/index.html.

1. Bennett, C.L. *et al.* The immune dysregulation, polyendocrinopathy, enteropathy, X-linked syndrome (IPEX) is caused by mutations of FOXP3. *Nat. Genet.* **27**, 20–21 (2001).
2. Fontenot, J.D., Gavin, M.A. & Rudensky, A.Y. Foxp3 programs the development and function of CD4+CD25+ regulatory T cells. *Nat. Immunol.* **4**, 330–336 (2003).
3. Hori, S., Nomura, T. & Sakaguchi, S. Control of regulatory T cell development by the transcription factor Foxp3. *Science* **299**, 1057–1061 (2003).
4. Zanin-Zhorov, A. *et al.* Protein kinase C-theta mediates negative feedback on regulatory T cell function. *Science* **328**, 372–376 (2010).
5. Collins, A.V. *et al.* The interaction properties of costimulatory molecules revisited. *Immunity* **17**, 201–210 (2002).
6. Yokosuka, T. *et al.* Spatiotemporal basis of CTLA-4 costimulatory molecule-mediated negative regulation of T cell activation. *Immunity* **33**, 326–339 (2010).
7. Teft, W.A., Kirchhof, M.G. & Madrenas, J. A molecular perspective of CTLA-4 function. *Annu. Rev. Immunol.* **24**, 65–97 (2006).
8. Kong, K.F. & Altman, A. In and out of the bull's eye: protein kinase Cs in the immunological synapse. *Trends Immunol.* **34**, 234–242 (2013).
9. Kong, K.F. *et al.* A motif in the V3 domain of the kinase PKC-theta determines its localization in the immunological synapse and functions in T cells via association with CD28. *Nat. Immunol.* **12**, 1105–1112 (2011).
10. Kim, J.K. *et al.* Impact of the TCR signal on regulatory T cell homeostasis, function, and trafficking. *PLoS ONE* **4**, e6580 (2009).
11. Park, S.G. *et al.* T regulatory cells maintain intestinal homeostasis by suppressing gammadelta T cells. *Immunity* **33**, 791–803 (2010).
12. Chuck, M.I., Zhu, M., Shen, S. & Zhang, W. The role of the LAT-PLC-gamma1 interaction in T regulatory cell function. *J. Immunol.* **184**, 2476–2486 (2010).
13. Spitaler, M., Emslie, E., Wood, C.D. & Cantrell, D. Diacylglycerol and protein kinase D localization during T lymphocyte activation. *Immunity* **24**, 535–546 (2006).
14. Wing, K. *et al.* CTLA-4 control over Foxp3+ regulatory T cell function. *Science* **322**, 271–275 (2008).
15. Qureshi, O.S. *et al.* Trans-endocytosis of CD80 and CD86: a molecular basis for the cell-extrinsic function of CTLA-4. *Science* **332**, 600–603 (2011).
16. Haribhai, D. *et al.* Regulatory T cells dynamically control the primary immune response to foreign antigen. *J. Immunol.* **178**, 2961–2972 (2007).
17. Tang, Q. & Bluestone, J.A. The Foxp3+ regulatory T cell: a jack of all trades, master of regulation. *Nat. Immunol.* **9**, 239–244 (2008).
18. Josefowicz, S.Z., Lu, L.F. & Rudensky, A.Y. Regulatory T cells: mechanisms of differentiation and function. *Annu. Rev. Immunol.* **30**, 531–564 (2012).
19. Matsuda, J.L. *et al.* Systemic activation and antigen-driven oligoclonal expansion of T cells in a mouse model of colitis. *J. Immunol.* **164**, 2797–2806 (2000).
20. Collison, L.W. *et al.* The inhibitory cytokine IL-35 contributes to regulatory T-cell function. *Nature* **450**, 566–569 (2007).
21. Shimizu, J., Yamazaki, S. & Sakaguchi, S. Induction of tumor immunity by removing CD25+CD4+ T cells: a common basis between tumor immunity and autoimmunity. *J. Immunol.* **163**, 5211–5218 (1999).
22. Fu, G. *et al.* Protein kinase C eta is required for T cell activation and homeostatic proliferation. *Sci. Signal.* **4**, ra84 (2011).
23. Tai, X. *et al.* Basis of CTLA-4 function in regulatory and conventional CD4+ T cells. *Blood* **119**, 5155–5163 (2012).
24. Kataoka, H. *et al.* CD25(+)CD4(+) regulatory T cells exert in vitro suppressive activity independent of CTLA-4. *Int. Immunol.* **17**, 421–427 (2005).
25. Onishi, Y., Fehervari, Z., Yamaguchi, T. & Sakaguchi, S. Foxp3+ natural regulatory T cells preferentially form aggregates on dendritic cells in vitro and actively inhibit their maturation. *Proc. Natl. Acad. Sci. USA* **105**, 10113–10118 (2008).
26. Tran, D.Q. *et al.* Analysis of adhesion molecules, target cells, and role of IL-2 in human FOXP3+ regulatory T cell suppressor function. *J. Immunol.* **182**, 2929–2938 (2009).
27. Sarris, M., Andersen, K.G., Randow, F., Mayr, L. & Betz, A.G. Neuropilin-1 expression on regulatory T cells enhances their interactions with dendritic cells during antigen recognition. *Immunity* **28**, 402–413 (2008).
28. Borsellino, G. *et al.* Expression of ectonucleotidase CD39 by Foxp3+ Treg cells: hydrolysis of extracellular ATP and immune suppression. *Blood* **110**, 1225–1232 (2007).
29. Zhao, Z.S., Manser, E., Loo, T.H. & Lim, L. Coupling of PAK-interacting exchange factor PIX to GIT1 promotes focal complex disassembly. *Mol. Cell. Biol.* **20**, 6354–6363 (2000).
30. Lucanic, M. & Cheng, H.J.A. RAC/CDC-42-independent GIT/PIX/PAK signaling pathway mediates cell migration in *C. elegans*. *PLoS Genet.* **4**, e1000269 (2008).
31. Phee, H., Abraham, R.T. & Weiss, A. Dynamic recruitment of PAK1 to the immunological synapse is mediated by PIX independently of SLP-76 and Vav1. *Nat. Immunol.* **6**, 608–617 (2005).
32. Ku, G.M., Yablonski, D., Manser, E., Lim, L. & Weiss, A.A. A Pak1-PIX-PKL complex is activated by the T-cell receptor independent of Nck, Slp-76 and LAT. *EMBO J.* **20**, 457–465 (2001).
33. Uhlig, H.H. *et al.* Characterization of Foxp3+CD4+CD25+ and IL-10-secreting CD4+CD25+ T cells during cure of colitis. *J. Immunol.* **177**, 5852–5860 (2006).
34. Dustin, M.L. T-cell activation through immunological synapses and kinapses. *Immunol. Rev.* **221**, 77–89 (2008).
35. Walker, L.S. & Sansom, D.M. The emerging role of CTLA4 as a cell-extrinsic regulator of T cell responses. *Nat. Rev. Immunol.* **11**, 852–863 (2011).
36. Read, S., Malmström, V. & Powrie, F. Cytotoxic T lymphocyte-associated antigen 4 plays an essential role in the function of Cd25+Cd4+ regulatory cells that control intestinal inflammation. *J. Exp. Med.* **192**, 295–302 (2000).
37. Tivol, E.A. *et al.* Loss of CTLA-4 leads to massive lymphoproliferation and fatal multiorgan tissue destruction, revealing a critical negative regulatory role of CTLA-4. *Immunity* **3**, 541–547 (1995).
38. Waterhouse, P. *et al.* Lymphoproliferative disorders with early lethality in mice deficient in Ctla-4. *Science* **270**, 985–988 (1995).
39. Buhlmann, J.E., Elkin, S.K. & Sharpe, A.H. A role for the B7–1/B7–2:CD28/CTLA-4 pathway during negative selection. *J. Immunol.* **170**, 5421–5428 (2003).
40. Ise, W. *et al.* CTLA-4 suppresses the pathogenicity of self antigen-specific T cells by cell-intrinsic and cell-extrinsic mechanisms. *Nat. Immunol.* **11**, 129–135 (2010).
41. Schneider, H. *et al.* Reversal of the TCR stop signal by CTLA-4. *Science* **313**, 1972–1975 (2006).
42. Rudd, C.E. The reverse stop-signal model for CTLA4 function. *Nat. Rev. Immunol.* **8**, 153–160 (2008).
43. Lu, Y., Schneider, H. & Rudd, C.E. Murine regulatory T cells differ from conventional T cells in resisting the CTLA-4 reversal of TCR stop-signal. *Blood* **120**, 4560–4570 (2012).
44. Peggs, K.S., Quezada, S.A. & Allison, J.P. Cancer immunotherapy: co-stimulatory agonists and co-inhibitory antagonists. *Clin. Exp. Immunol.* **157**, 9–19 (2009).
45. Peggs, K.S., Quezada, S.A., Chambers, C.A., Korman, A.J. & Allison, J.P. Blockade of CTLA-4 on both effector and regulatory T cell compartments contributes to the antitumor activity of anti-CTLA-4 antibodies. *J. Exp. Med.* **206**, 1717–1725 (2009).

ONLINE METHODS

Antibodies and reagents. mAbs specific for mouse CD3 (clone 145-2C11), CD28 (clone 37.51) or CTLA-4 (clone UC10-4B9) were purchased from Biolegend, as were fluorophore-conjugated anti-CD4 (clone GK1.5), anti-CD8 (53-6.7), anti-Foxp3 (clone FJK-16s), anti-CD25 (clone PC61), anti-CD44 (clone IM7) and anti-GITR (clone DTA-1) mAbs. Anti-human CD3 mAb (OKT3) was purified in-house. Polyclonal anti-PKC-θ (sc-212), anti-PKC-η (C-15 and sc-215), anti-PAK (N-20 and sc-882), anti-NFATc1 (7A6), anti-lamin B (M-20) and anti–α-tubulin (TU-02) Abs were obtained from Santa Cruz Biotechnology. Anti-p65 (NF-κB), anti-GIT2 and anti-αPIX Abs were obtained from Cell Signaling Technology. Anti-Foxp3 Abs (clone 150D/E4 for immunoblotting and clone FJK-16s for flow cytometry) were purchased from eBiosciences. Alexa Fluor 647–conjugated anti-mouse Ig and Alexa Fluor 555–conjugated anti-rabbit Ig were obtained from Molecular Probes. Digitonin was obtained from EMD Chemicals. Calf intestinal alkaline phosphatase was purchased from New England BioLabs. Recombinant CD86-Fc was previously described[46].

Plasmids. Plasmids of full-length human *Prkch* and mouse *Ctla4* were generated via PCR amplification and cloned into the pEF4/HisC expression vector or pMIG retroviral vector, respectively. *Prkch* and *Ctla4* point mutations were generated using Quikchange II Site-directed Mutagenesis Kit (Stratagene). *Ctla4* mutants encoding variants with cytoplasmic tail deletions (amino acids 183–223 and 192–223) were generated via PCR amplification.

Mice and primary cell cultures. C57BL/6 (B6; CD45.2$^+$), B6.SJL (CD45.1$^+$) and *Prkch*$^{-/-}$ (CD45.2$^+$)[22] mice were housed and maintained under specific pathogen–free conditions, and manipulated according to guidelines approved by the LIAI Animal Care Committee and the Animal Care and Use Committee of The Scripps Research Institute. The *Prkch*$^{-/-}$ mice are now available from the Jackson Laboratories (B6.Cg-Prkch<tm1.1Gasc>/J). *Foxp3*-IRES-eGFP (FIG) mice were obtained from the Jackson Laboratories. *Prkch*$^{-/-}$ × *Foxp3*-IRES-eGFP (*Prkch*$^{-/-}$ FIG) mice[16] were generated by crossing FIG mice with *Prkch*$^{-/-}$ mice[22]. 8–12-week-old mice with no preference for genders were used. CD4$^+$ T cells were isolated by anti-CD4 (BD Biosciences) positive selection, and were cultured in RPMI-1640 medium (Mediatech, Inc.) supplemented with 10% heat-inactivated FBS, 2 mM glutamine, 1 mM sodium pyruvate, 1 mM MEM nonessential amino acids, and 100 U/ml each of penicillin G and streptomycin (Life Technologies).

Immunoprecipitation and immunoblotting. Simian virus 40 large T antigen-transfected human leukemic Jurkat T cells (JTAg) and MCC-specific hybridoma T cells have been described previously[9]; these cell lines have not been recently short tandem repeat–profiled but tested negative for mycoplasma contamination. JTAg cells in logarithmic growth phase were transfected with plasmid DNAs by electroporation and incubated for 48 h. Transfected cells were stimulated with an anti-human CD3 (OKT3) mAb plus recombinant CD86-Fc and a cross-linking Ab (JTAg) or anti-CTLA-4 mAb (T hybridoma) for 5 min. Cell lysis in 1% NP-40 lysis buffer (50 mM Tris-HCl, 50 mM NaCl and 5 mM EDTA), immunoprecipitation and immunoblotting were carried out as previously described[9].

Enzyme-linked immunosorbent assay. Serum IgE was quantified using capture and biotinylated mAbs from CALTAG Laboratories, as previously described[47]. Autoantibodies specific for double-stranded DNA (dsDNA) and histone were determined using plates coated with salmon sperm DNA (Life Technologies) or calf thymus histone (Roche), respectively. Detection was carried out using biotinylated anti-mouse IgG, streptavidin conjugated HRP and ABTS substrates (Bio-Rad). Relative Ig serum titers were calculated by dividing the absorbance values of experimental samples by the negative control values.

Isolation of mRNA, cDNA synthesis and real-time PCR. Total RNA was extracted from sorted CD4$^+$GFP$^-$ and CD4$^+$GFP$^+$ cells of FIG mice using the RNeasy kit (Qiagen). RNA was used to synthesize cDNA by the SuperScript III FirstStrand cDNA synthesis kit (Life Technologies). Gene expression was determined using real-time PCR with iTaq SYBR Green (Bio-Rad) in the presence of the following primer sets for mouse *Ctla4* (forward: 5′-ACTCATGTACCCACCGCCATA-3′; reverse: 5′-GGGCATGGTTCTGGATCAAT-3′), *Prkch* (forward: 5′-CAAGC ATTTTACCAGGAAGCG-3′; reverse: 5′-TGTTTCCCAAATACTCCCCAG-3′) and the housekeeping gene β-actin (*Actb*). Relative gene expression levels were determined in triplicates and calculated using the $2^{-\Delta\Delta Ct}$ and normalized to the abundance of *Actb*.

Microscopy. CD4$^+$ T cells were purified from moth cytochrome C (MCC)–specific mice expressing the transgenic AND TCR crossed with *Rag2*$^{-/-}$ (AND-Tg × *Rag2*$^{-/-}$) mice and stimulated by immobilized anti-CD3ε (145-2C11; 10 μg/ml) and anti-CD28 (PV-1; 1 μg/ml) in the presence of mouse recombinant IL-2 (10 ng/ml) and human recombinant TGFβ (5 ng/ml) for 3 d. The cells were retrovirally transduced with vectors encoding eGFP-tagged mouse PKC-θ or PKC-η for 24 h 1 d after the initial stimulation. On day 4 or later, the cells were sorted on a FACSAria (BD) to obtain purified (≥90%) GFP$^+$ cells, which were maintained in culture. B cells purified from B10.BR mice and stimulated by LPS (Difco; 10 μg/ml) plus MCC (1 μM) were added to the cultured T cells for 1 d. Dead cells were removed by Lympholite-M (Cedarlane), and the CD4$^+$ T_{reg} cells were prestained by DyLight650-labeled anti-TCRβ (H57) Fab, conjugated with MCC-pulsed LPS-stimulated B cells for 5–10 min, fixed with 2% PFA, and imaged by confocal microscopy (Leica SP5) with ProLong gold antifade reagent with DAPI (Molecular Probes).

***In vitro* suppression assay.** Flow cytometry–sorted naive CD4$^+$CD62L$^+$ T_{eff} cells were labeled with 5 μM of CellTrace Violet according to the manufacturer's protocol (Life Technologies). CD11c$^+$ splenic DCs were purified according to the manufacturer's instructions (Miltenyi Biotech). Labeled T_{eff} cells (2×10^4) and splenic DCs (5×10^3) were cocultured for 3 d with CD4$^+$GFP$^+$ T_{reg} cells (0.125×10^4 to 4×10^4) sorted from *Prkch*$^{+/+}$ or *Prkch*$^{-/-}$ FIG mice in the presence of an anti-mouse CD3 mAb.

Homeostatic expansion model. Naive CD4$^+$CD62L$^+$ cells from congenic B6.SJL (CD45.1$^+$) and CD4$^+$GFP$^+$ T_{reg} (CD45.2$^+$) cells from *Prkch*$^{+/+}$ and *Prkch*$^{-/-}$ FIG mice were sorted using ARIA Cell Sorter (BD Biosciences). Two × 10^6 naive T cells were transferred intravenously alone or together with 0.5×10^6 CD4$^+$GFP$^+$ T_{reg} cells into *Rag1*$^{-/-}$ mice; this was done in a blinded fashion and assigned randomized with no pre-established inclusion or exclusion criteria. Mice were killed 7–10 d after transfer. Spleens, peripheral lymph nodes and mesenteric lymph nodes were harvested, and each population was independently analyzed by flow cytometry. To achieve reasonable power, at least 5 mice/group (15 mice/experiment) were used. Additional mice were added to experiments as appropriate.

B16 melanoma model. Splenocytes from normal B6 mice were depleted of CD25$^+$ cells using biotinylated anti-CD25 mAb (clone PC61, eBiosciences) and streptavidin-conjugated beads (BD Biosciences). CD4$^+$GFP$^+$ T_{reg} cells were sorted using flow cytometry from *Prkch*$^{+/+}$ or *Prkch*$^{-/-}$ FIG mice. 15×10^6 CD25-depleted splenocytes were adoptively transferred alone or together with 0.5×10^6 *Prkch*$^{+/+}$or *Prkch*$^{-/-}$ CD4$^+$GFP$^+$ T_{reg} cells into recipient *Rag1*$^{-/-}$ mice; this was done in a blinded fashion and assigned in a randomized fashion with no pre-established inclusion or exclusion criteria. 2×10^5 B16-F10 melanoma cells were inoculated intradermally on the right shaved flank the next day. Tumor size was measured using an electronic dial caliper 2–3 times/week[14]. To achieve reasonable power, at least 5 mice/group (15 mice/experiment) were used. Additional mice were added to experiments as appropriate.

BM chimeras. cDNAs encoding full-length human wild-type or S28A,S32A substituted *Prkch* were subcloned into a modified pMIG retroviral vector containing IRES and non-signaling rat CD2 gene (lacking the cytoplasmic tail). BM chimeras were produced in irradiated B6 mice as previously described[9]. Briefly, BM cells were flushed from the femurs and tibias of *Prkch*$^{-/-}$ FIG mice that have been pretreated with 5-fluorouracil to enrich for stem cells. BM cells were cultured in DMEM (Mediatech, Inc.) containing 10% FBS, IL-3 (20 ng/ml), IL-6 (25 ng/ml) and stem cell factor (SCF; 100 ng/ml). Retroviral infections were carried out for two consecutive days. 1×10^6 infected BM cells were intravenously injected into irradiated B6 mice. Analyses were performed

10–12 weeks after reconstitution to determine cells coexpressing GFP (for Foxp3 expression) and rat CD2 (for transgene expression) using anti-rCD2 mAb (clone OX-34, Biolegend). Cells were pooled from spleens and peripheral LN of 4–5 chimeric mice, and enriched for $CD4^+$ cells. GFP^+rCD2^+ double-positive T_{reg} cells were sorted on an ARIA Cell Sorter, and their *in vivo* suppressive function was analyzed in a homeostatic expansion assay as described above.

T_{reg} cell–APC coculture. GFP^+ T_{reg} cells (5×10^4) from *Prkch*$^{+/+}$ or *Prkch*$^{-/-}$ FIG mice were cultured with CellTrace Violet-labeled splenic $CD11c^+$ APCs (5×10^4) for the indicated times. Cells were carefully collected with cut tips and immediately assayed on an LSRII flow cytometer to determine double-positive ($GFP^+Violet^+$) conjugates. For the CD86 depletion experiment, T_{reg} cells (5×10^4) were cultured with $CD45.2^+CD11c^+$ splenic DCs (2.5×10^4) for 9 h, followed by addition of $CD45.1^+CD11c^+$ splenic DCs (2.5×10^4) from B6.SJL mice for another 9 h. Cells were collected at different time points and stained with fluorophore-conjugated Abs specific for CD11c, Annexin V, CD4, CD86, I-A^b, CD45.1 or CD45.2.

Stable isotope labeling by amino acids in cell culture and phosphoproteomic analysis. *Prkch*$^{+/+}$and *Prkch*$^{-/-}$ FIG naive $CD4^+$ T cells were differentiated into iT_{reg} cells as described above in regular RPMI-1640 medium or medium supplemented with ^{13}C and ^{15}N–labeled lysine and arginine for stable isotope labeling by amino acids in cell culture (SILAC) labeling. GFP^+ T_{reg} cells sorted by flow cytometry were left unstimulated or stimulated with anti-CD3 plus anti–CTLA-4 mAbs for 5 min. *Prkch*$^{+/+}$ and *Prkch*$^{-/-}$ FIG cell lysates were mixed at a 1:1 ratio, and 300 µg of the protein mixture was precipitated with 5x volume of cold acetone. After centrifugation at 14,000*g* (10 min at 4 °C), protein pellets were solubilized and reduced with 100 mM Tris-HCl, 8 M urea and 5 mM tris(2-carboxyethyl)phosphine. Cysteine was alkylated with 10 mM iodoacetamide. The solution was diluted 1:4 and digested with 5 µg of trypsin at 37 °C overnight. Digestion was terminated by adding 10% acetonitrile and 2% formic acid, and the resulting peptides were subjected to TiO_2 phosphopeptide enrichment as described[48]. Briefly, phosphopeptides were bound to the TiO_2 resin, and eluted with 250 mM NH_4HCO_3, pH 9. Enriched phosphopeptides were analyzed by the MudPIT LC-MS/MS method[49]. MS analysis was performed using an LTQ-Orbitrap Velos mass spectrometer (Thermo Fisher). A cycle of one full-scan mass spectrum (300–1,800 *m/z*) at a resolution of 60,000 followed by 20 data-dependent MS/MS spectra at a 35% normalized collision energy was repeated continuously throughout each step of the multidimensional separation.

MS data were analyzed by the Integrated Proteomics Pipeline IP2 (Integrated Proteomics Applications; http://www.integratedproteomics.com/). The tandem mass spectra were searched against the European Bioinformatics Institute's International Protein Index mouse target-decoy protein database. Protein false discovery rates were controlled below 1% for each sample. In ProLuCID database search, the cysteine carboxyamidomethylation was set as a stable modification, and phosphorylation on serine, threonine or tyrosine was configured as differential modification. Peptide quantification was performed by Census software, in which the isotopic distributions for both the unlabeled and labeled peptides were calculated and this information was then used to determine the appropriate mass-to-charge ratio (*m/z*) range from which to extract ion intensities. Phosphopeptides were further evaluated with IP2 phospho analysis module, which computes Ascore[50] and Debunker score[51].

Statistical analysis. Statistical analyses were performed using, unless otherwise stated, analysis of variance (ANOVA) with post hoc Bonferroni's corrections. Unless otherwise indicated, data represent the mean ± s.e.m., with $P < 0.05$ considered statistically significant.

46. Kim, G. *et al.* Spontaneous colitis occurrence in transgenic mice with altered B7-mediated costimulation. *J. Immunol.* **181**, 5278–5288 (2008).
47. Becart, S. *et al.* SLAT regulates Th1 and Th2 inflammatory responses by controlling Ca2+/NFAT signaling. *J. Clin. Invest.* **117**, 2164–2175 (2007).
48. Wang, H. *et al.* The interaction of CtIP and Nbs1 connects CDK and ATM to regulate HR-mediated double-strand break repair. *PLoS Genet.* **9**, e1003277 (2013).
49. Washburn, M.P., Wolters, D. & Yates, J.R. III. Large-scale analysis of the yeast proteome by multidimensional protein identification technology. *Nat. Biotechnol.* **19**, 242–247 (2001).
50. Beausoleil, S.A., Villen, J., Gerber, S.A., Rush, J. & Gygi, S.P. A probability-based approach for high-throughput protein phosphorylation analysis and site localization. *Nat. Biotechnol.* **24**, 1285–1292 (2006).
51. Lu, B., Ruse, C., Xu, T., Park, S.K. & Yates, J. III. Automatic validation of phosphopeptide identifications from tandem mass spectra. *Anal. Chem.* **79**, 1301–1310 (2007).

doi:10.1038/ni.2866

Erratum: Protein kinase C-η controls CTLA-4–mediated regulatory T cell function

Kok-Fai Kong, Guo Fu, Yaoyang Zhang, Tadashi Yokosuka, Javier Casas, Ann J Canonigo-Balancio, Stephane Becart, Gisen Kim, John R Yates III, Mitchell Kronenberg, Takashi Saito, Nicholas R J Gascoigne & Amnon Altman
***Nat. Immunol.* 15, 465–472; published online 6 April 2014; corrected after print 2 May 2014**

In the version of this article initially published, the second affiliation for Nicholas R.J. Gascoigne was incorrect. The correct affiliation is The Department of Microbiology, Yong Loo Lin School of Medicine, National University of Singapore, Singapore. The error has been corrected in the HTML and PDF versions of the article.